

AD-603 0611

Top

ONR TECHNICAL REPORT NO. 69

Project: NR 356-378

Contract: Nonr 3357(01)

34 p 42 x 60  
\$ 0.00

THE MEASUREMENT OF THE ORIENTATION RATE  
OF CRYSTALS IN A CRYSTALLINE POLYMER BY  
DYNAMIC X-RAY DIFFRACTION\*

May 22, 1964

H. Kawai, T. Itoh, D. A. Keedy, and R. S. Stein  
POLYMER RESEARCH INSTITUTE  
University of Massachusetts, Amherst, Massachusetts

Best Available Copy

THE MEASUREMENT OF THE ORIENTATION RATE  
OF CRYSTALS IN A CRYSTALLINE POLYMER BY  
DYNAMIC X-RAY DIFFRACTION<sup>†</sup>

H.Kawai<sup>\*</sup>, T.Itoh<sup>\*</sup>, D.A.Keedy, and R.S.Stein

POLYMER RESEARCH INSTITUTE

University of Massachusetts, Amherst, Massachusetts

INTRODUCTION

Dynamic birefringence measurements on crystalline polymers such as polyethylene indicate that there is a characteristic time for change in molecular orientation (of the order of a second for polyethylene at room temperature<sup>1,2</sup>). This time has been ascribed to that required for crystals to change their orientation following the deformation of the polymer. In order to test this proposal a direct measurement of this orientation time by x-ray diffraction during the steady state vibrational strain of the sample was attempted.

The measurement was carried out by an "x-ray stroboscope" principle in which the intensity of the diffracted x-rays was measured during a small part of the vibration period but repeated during successive period.

This may be illustrated using (Fig. 1) in which the variation of strain with time and also the variation of the intensity of x-ray diffraction at a particular set of diffraction angles during periodic strain of a sample are plotted for a hypothetical crystalline polymer. In general, the intensity of diffraction will vary as the sample is strained as a result, in part, of the change in crystal orientation with strain. However, the amount of such change may depend upon sample type, vibration frequency, and temperature. Also, the diffraction change may lead or lag the strain in phase.

---

<sup>†</sup>Supported in part by grants from the Petroleum Research Fund and the Air Force Office of Scientific Research and the Army Research Office (Durham) and by contracts from the Office of Naval Research

<sup>\*</sup>On leave from the Department of Polymer Chemistry, Kyoto Univ., Kyoto, Japan, on an International Grant from the Petroleum Research Fund of the American Chemical Society.

<sup>\*</sup>On leave from the Department of Polymer Chemistry, Kyoto University, Kyoto, Japan

A detector for diffracted x-rays is now arranged to only count during the interval labeled "A" on Fig. (1) and to do so repetitively at the corresponding time interval during a sufficient number of periods of vibration to assure statistical significance. The detector may simultaneously count during the interval "B" of Fig. (1), sending its signal to a second channel. Additional counting channels are employed in practice.

Then the variation of accumulated count with the azimuthal angle,  $\phi$ , of Fig. (2) is measured simultaneously for all counting channels and done so for each frequency of sample vibration. If there is no change in crystal orientation or diffracting ability in the course of the vibration, all sample channels should give identical results. The difference between results actually obtained among the channels is a measure of the amount of change in orientation in the corresponding time intervals.

#### EXPERIMENTAL

The apparatus, shown diagrammatically in Fig. (3), is constructed on a lathe bed. A General Electric XRD-6 75 K.V.P. generator powers a G.E. Type EA-75 tube which is mounted horizontally on the lathe bed. This provides a high energy but comparatively broad source of x-rays which is collimated using a slit system providing a beam 0.2 cm wide x 1.4 cm high in dimensions at the sample with a horizontal angular divergence of  $\pm 0.5^\circ$  and a vertical divergence of  $\pm 2^\circ$ . A diagrammatic sketch of the collimating system is given in Fig. 4. The x-ray tube is mounted on a plate which may slide horizontally on a base plate and which may be rotated with respect to the sample axis in order to adjust the angle of incidence for the x-rays.

The sample is mounted in a vibrator (Fig. 5) which permits one to vary the azimuthal angle while the sample is subjected to tensile vibration.<sup>\*</sup> This is powered by a 1 H.P. D.C. motor and Ratiotrol<sup>†</sup> electronic variable speed control. Through use of this and an arrangement of gears and timing belts, continuously variable speeds

---

<sup>\*</sup>Manufactured by Iwamoto Seisakusho Inc., Kyoto, Japan

<sup>†</sup>Boston Gear Company, Boston, Massachusetts

between 0.01 and 20 revolutions per second may be provided. By rotation of pairs of eccentric cams, the vibrator produces linear vibration of the both sample jaws at strain amplitudes of 0.08, 0.1, 0.4, and 0.8 cm. The circular plate holding the cam and jaw assembly may be rotated through  $360^\circ$  of azimuthal angle while the sample is vibrating, by manually rotating a drive shaft and worm gear which engages with gear teeth on the periphery of this plate. Provision is made so that a motor drive for this azimuthal angular adjustment may be provided for automatic scanning.

The sample, usually 2 cm x 4 cm x 0.03 cm dimension is mounted between clamps which can be adjusted, by means of a screw, with respect to the drive rod from the cam assembly so as to provide a static strain. The application of such a static strain is necessary to prevent slackening of the sample during the minimum strain part of the vibration. By adjusting sample lengths and replacing cams, it is possible to achieve vibrational strain of 0-40% amplitude superposed on static strains of 0-100%.

The diffracted radiation is detected by a Philips 63019 Geiger tube provided with Soller slits and knife-edge slit collimators limiting the angular divergence to  $\pm 0.50^\circ$ . The geiger tube is mounted on an arm which may be manually adjusted to a selected Bragg angle corresponding to diffraction from the crystal plane under study. The geiger tube is shock mounted so that its center wire is not caused to vibrate by the sample vibration. (It has been decided that a proportional counter would be a superior detector because of its shorter resolving time. Even though the average counting rate is low, the high instantaneous counting rate during the short counting interval when a particular channel is activated approaches values where coincidence errors are appreciable.)

The amplified<sup>+</sup> output of the geiger tube is distributed to four scalers<sup>\*</sup> by an electronic gating circuit activated by signals received from a commutator rotating in synchronism with the sample vibrator. Each scaler is activated during a fraction of the vibrational period determined by the setting of the commutator.

---

<sup>+</sup>Tracerlab Pulse Amplifier

<sup>\*</sup>Berkeley Decimal Scaler, Model 2000

The commutator, seen in Fig. 5, consists of a number of cams mounted on a common shaft which is rotated by the sample vibration mechanism. Each cam trips a microswitch as it rotates which controls a signal to the gating circuit. The cams are constructed so that the time interval during which the microswitch is closed and its phase relationship to the strain ( $t_A$  and  $\Delta t_A$  of Fig. 1) is adjustable. (It is found that at the higher vibration frequencies, the time interval for microswitch closure is comparable with  $\Delta t_A$  giving rise to a timing error.\* The commutator will be replaced by a photoelectrically operated mechanism in an improved apparatus).

The entire diffractometer is enclosed in a lead-lined wooden box to protect the operators from stray radiation. Temperature control for the sample will be provided in the improved apparatus.

#### OPERATION OF APPARATUS

The collimating system for the incident beam was carefully aligned, first using a traveling microscope and then by taking photographs of the x-ray beam at various positions. In this way, it was ascertained that the beam passed through the center of the sample located at the center of rotation of the detector arm.

The operation of the commutator, gating circuit and scalers was checked by feeding in pulses from a signal generator and observing the number of pulses recorded by each scaler as a function of the number of revolutions per second of the commutator. With 1610 pulses per second input, it was found that the measured fraction of the total counts recorded by each channel remained constant and was reproducible to about  $\pm 2\%$  up to commutator speeds of 20 cycles per second (when each channel counts for 4% of the time for a revolution of the commutator). However, with a lower pulse rate of 165 per second, the error increased to  $\pm 5\%$  at the higher frequencies.

The counting system was also checked using the geiger tube with a radioactive source and it was found to function properly within the precision expected on the basis of the statistical and coincidence errors expected on the basis of the total number of counts and counting rates.

An attempt was made to correct this error by making counts as a function of frequency with a constant intensity signal from the attenuated incident x-ray beam using the same microswitch.

The resolution of the apparatus in the direction of the Bragg angle was checked by making a scan on a quenched unoriented sample of an experimental medium density polyethylene film giving the results plotted in Fig. 6. The azimuthal dependence results presented in Figures 7 through 13 are at the Bragg angle of  $\theta = 10.6^\circ$  corresponding to the 110 peak. 50KV, 50 ma Ni-filtered CuK $\alpha$  radiation was used throughout.

### RESULTS

The variation of the intensity of the 110 peak with azimuthal angle for the static variation of intensity for samples elongated 20% and 30% are shown in Fig. 7. One finds the usual results that the crystal orientation is greatest at a small angle to the machine direction, and that the orientation distribution becomes sharper at the higher strain.

If the sample is vibrated at large amplitude, it will become slack during the minimum strain part of the vibration cycle unless the static strain is sufficient so that the time required for contraction of the sample is less than the half-period of vibration. This slackening is undesirable since the sample then moves with respect to the x-ray beam disorting the diffraction angles and intensities. The required static strain to prevent slackening becomes greater with increasing vibration frequency as shown in Fig. 8. This also depends upon the dynamic strain amplitude and upon the thermal treatment of the sample during preparation and study.

The possibility that dynamic vibration of the sample might produce changes of orientation or of dynamic behavior with time was studied by examining the sample after many thousands of cycles of vibration. Changes occur during the early stages of dynamic straining after which there is negligible additional fatigue. For example, the azimuthal variation of intensity of the 110 peak for a sample given a static strain of 30% is shown after 0, 100, 500, 1000 and 5000 cycles of 5% strain amplitude dynamic

strain in Fig. 9.

Dynamic studies were carried out at vibration frequencies of 0.01, 1, 10, and 20 cycles per second at static strain of 20% and dynamic strain amplitudes of 5% and 2.5% and are presented in Figures (10) and (13). The data are compared with the azimuthal variation measured for static deformations. That is, for example, the solid and dotted lines of Fig. 12 are for measurements of the azimuthal intensity variations for films held elongated 20 and 25%, while the points represent measurements made during vibration at times corresponding to minimum strain of 20% and maximum strain of 25%. The change of strain during the counting time interval at these strains was of the order of 0.2%.

It is seen in Figures (10) and (11) that at the lower vibration frequencies, there is little difference between the static and dynamic measurements. Consequently, the 110 plane of the crystal can change its orientation in times shorter than the corresponding vibration periods of 100 seconds and 1 second, respectively.

In Figures (12) and (13), however, it is seen that there is increasing difference between the static and dynamic data at the higher frequencies of 10 and 20 c.p.s. with perhaps a 20-30% difference at 20 c.p.s. It is believed that this difference is considerably outside of experimental error and that this represents the expected dispersion resulting from a crystal orientation time of the order of 0.1 sec., in qualitative agreement with birefringence results.

The present experiments at frequencies of 20 c.p.s. are at the maximum frequency for satisfactory performance of the apparatus. The extension to higher frequencies which is obviously desirable is dependent upon a redesign of the commutator dispensing with the microswitches. The measurements are being extended to lower temperatures (where the crystal orientation time is longer) and to other Bragg angles (in order to characterize the orientation of other crystal planes).

In this experiment the technique comparing dynamic x-ray diffraction intensities with static intensities at maximum and minimum strain of the sample and detecting

a characteristic (relaxation) time for polymer crystal orientation was used. An alternate technique comparing dynamic diffraction intensity at lag phase with that at lead phase of sample angle from maximum or minimum strain, as shown in Figure (14) by open circles of  $\pm \delta'$  or  $\pm \delta$ , can also be used. The latter technique may be more sensitive and more easily used than the former for detecting a characteristic time for crystal orientation behavior, being relatively free from the effect of accumulated cycles (fatigue) when the diffraction measurement is carried out at a particular azimuthal angle.

These dynamic x-ray diffraction techniques are not only available for determination of characteristic times for crystal orientation or deformation from dynamic measurements of x-ray diffraction intensity along the azimuthal or Bragg angle as function of frequency at a constant temperature, but also useful for determination of rates of reversible strain-induced crystallization, reversible strain-induced crystal transitions, and rates of migration of crystal dislocations, twin-boundaries and stacking faults.



# REFERENCES

- 1) R. S. Stein, S. Onogi, K. Sasaguri and D. A. Keedy, J. Appl. Phys. 34, 80, (1963)
- 2) K. Sasaguri and S. Hoshino and R. S. Stein, J. Appl. Phys. 35 47 (1964)

## FIGURES

1. The principle of the dynamic diffractometer.
2. The diffraction angle.
3. A diagrammatic sketch of the dynamic diffractometer.
4. A diagrammatic sketch of the collimating system.
5. A photograph of the vibrator.
6. The variation of diffracted intensity with Bragg angle for a quenched medium density polyethylene film.
7. The variation of diffracted intensity with azimuthal angle for the 110 peak of the above film stretched statically 20% and 30%.
8. The dependence of the required static strain to prevent sample slackening on vibration frequency for polyethylene films.
9. The azimuthal variation of the diffracted intensity of the 110 peak of polyethylene at 30% static strain after 0, 500, 1000, and 5000 cycles of dynamic strain at a rate of 1 c.p.s. between 20 and 30% strain.
10. A comparison of the azimuthal variation of intensity for a polyethylene sample under static strain with one subjected to dynamic strain of 5% with a static strain of 20% at a frequency of 0.01 c.p.s.
11. A comparison of the azimuthal variation of intensity for a polyethylene sample under static strain with one subjected to dynamic strain of 2.5% with a static strain of 20% at a frequency of 1 c.p.s.
12. A comparison of the azimuthal variation of intensity for a polyethylene sample under static strain with one subjected to dynamic strain of 2.5% with a static strain of 20% at a frequency of 10 c.p.s.
13. A comparison of the azimuthal variation of intensity for a polyethylene sample under static strain with one subjected to dynamic strain of 2.5% with a static strain of 20% at a frequency of 20 c.p.s.
14. Dynamic strain - phase diagram.

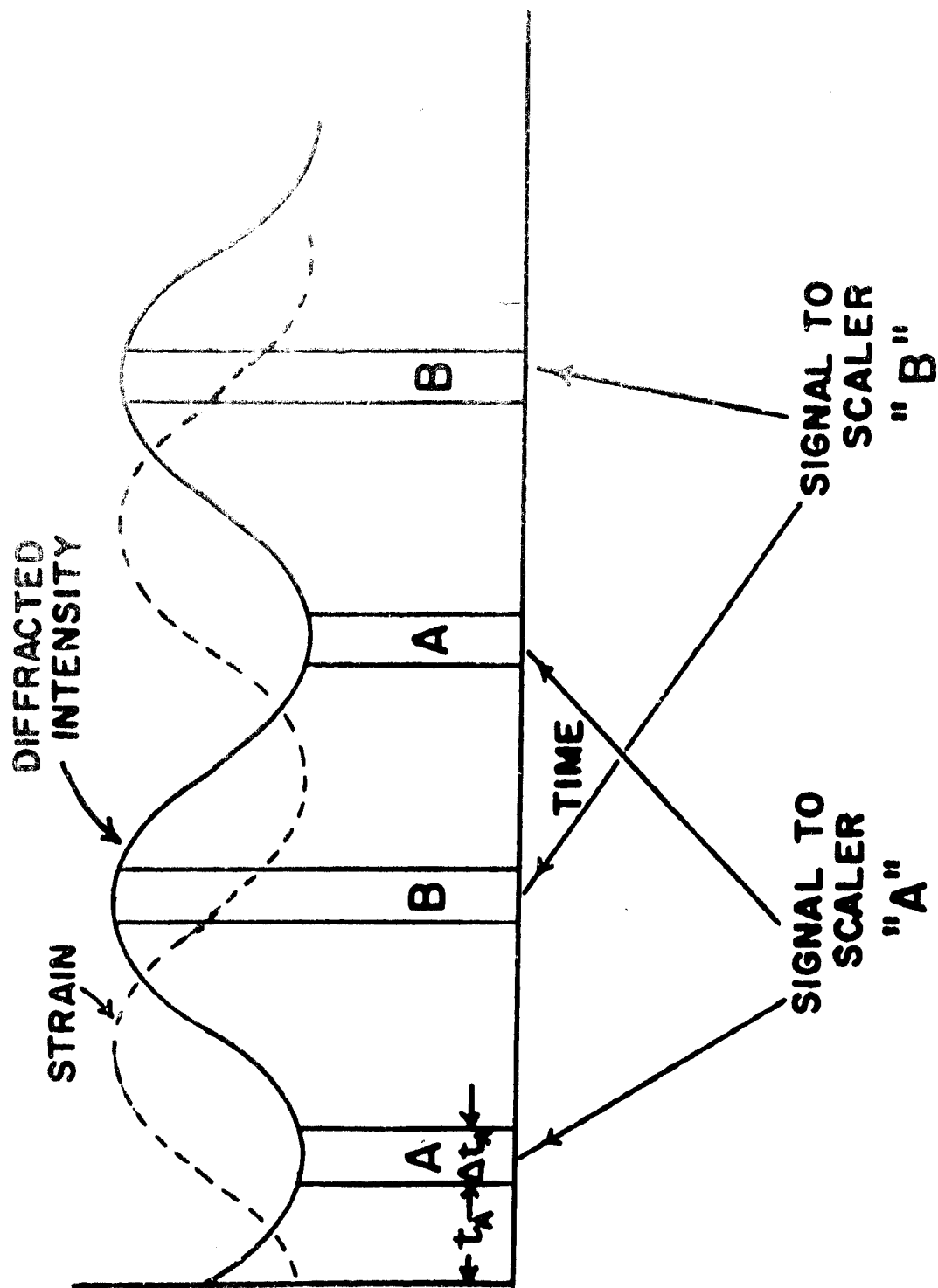
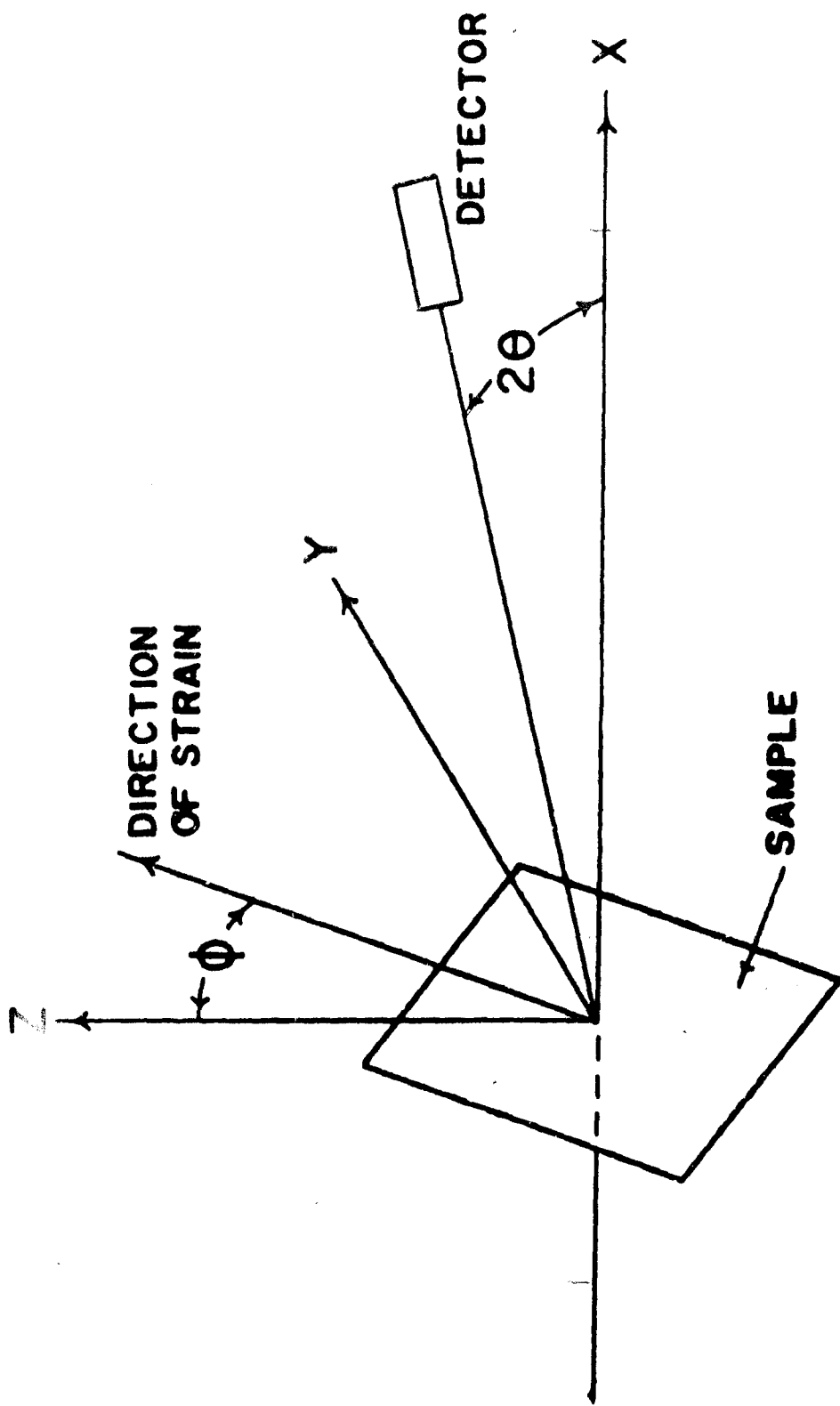


Figure 1



**Figure 2**

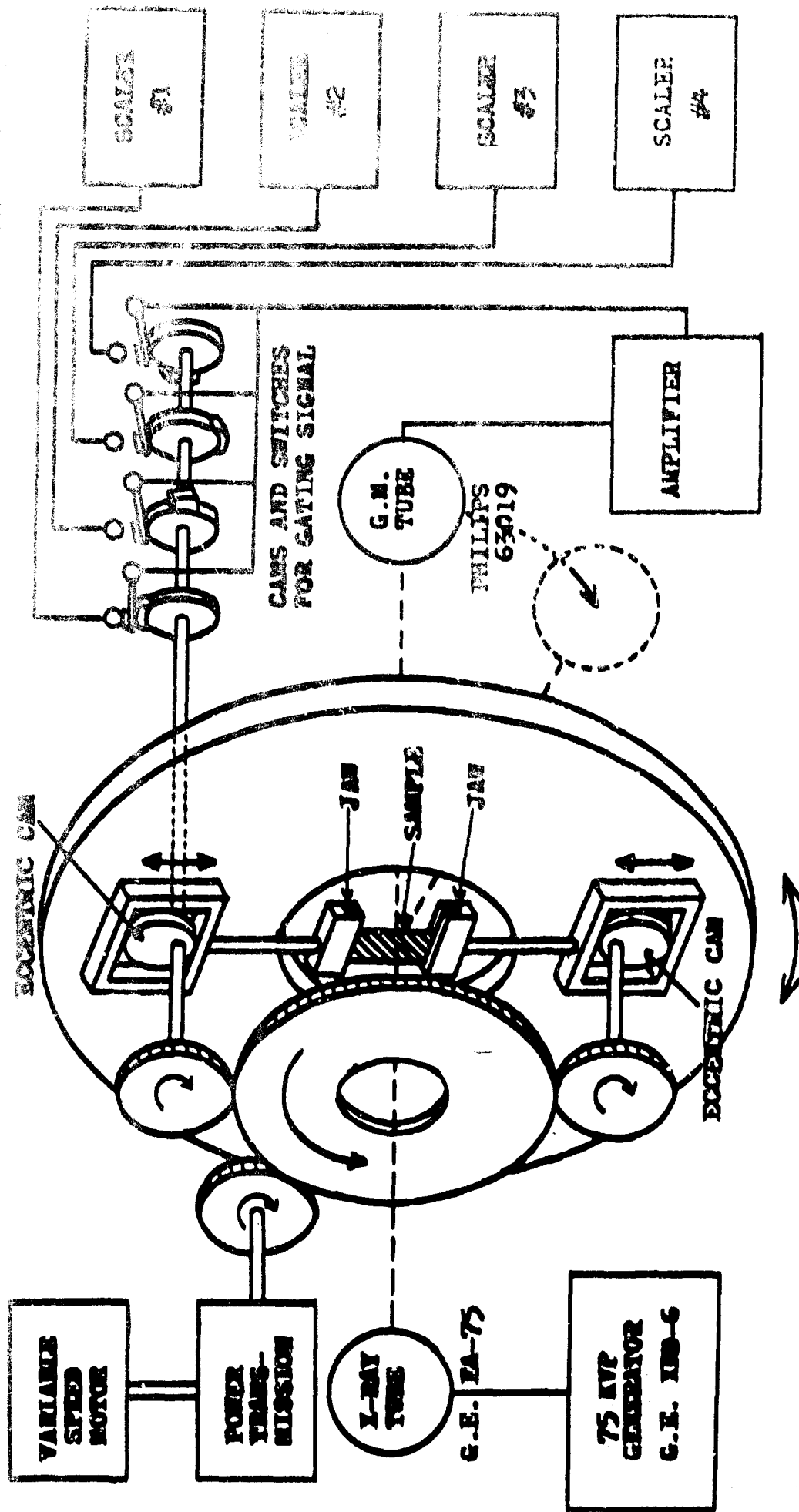
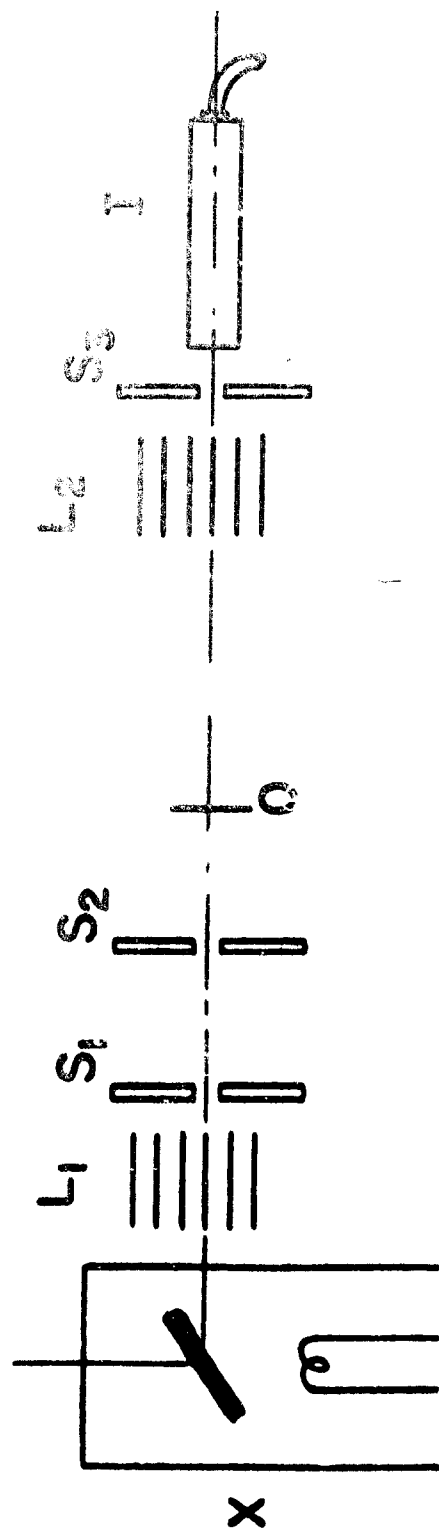


Figure 3



**X : X-RAY TUBE (EA-75, G.E.)**  
**L<sub>1</sub>, L<sub>2</sub> : SOLLER SLITS**  
**S<sub>1</sub>, S<sub>2</sub>, S<sub>3</sub> : SLIT SYSTEM**  
**O : AXIS OF THE GONIOMETER**  
**I : G.M. TUBE (PHILIPS)**

**Figure 4**

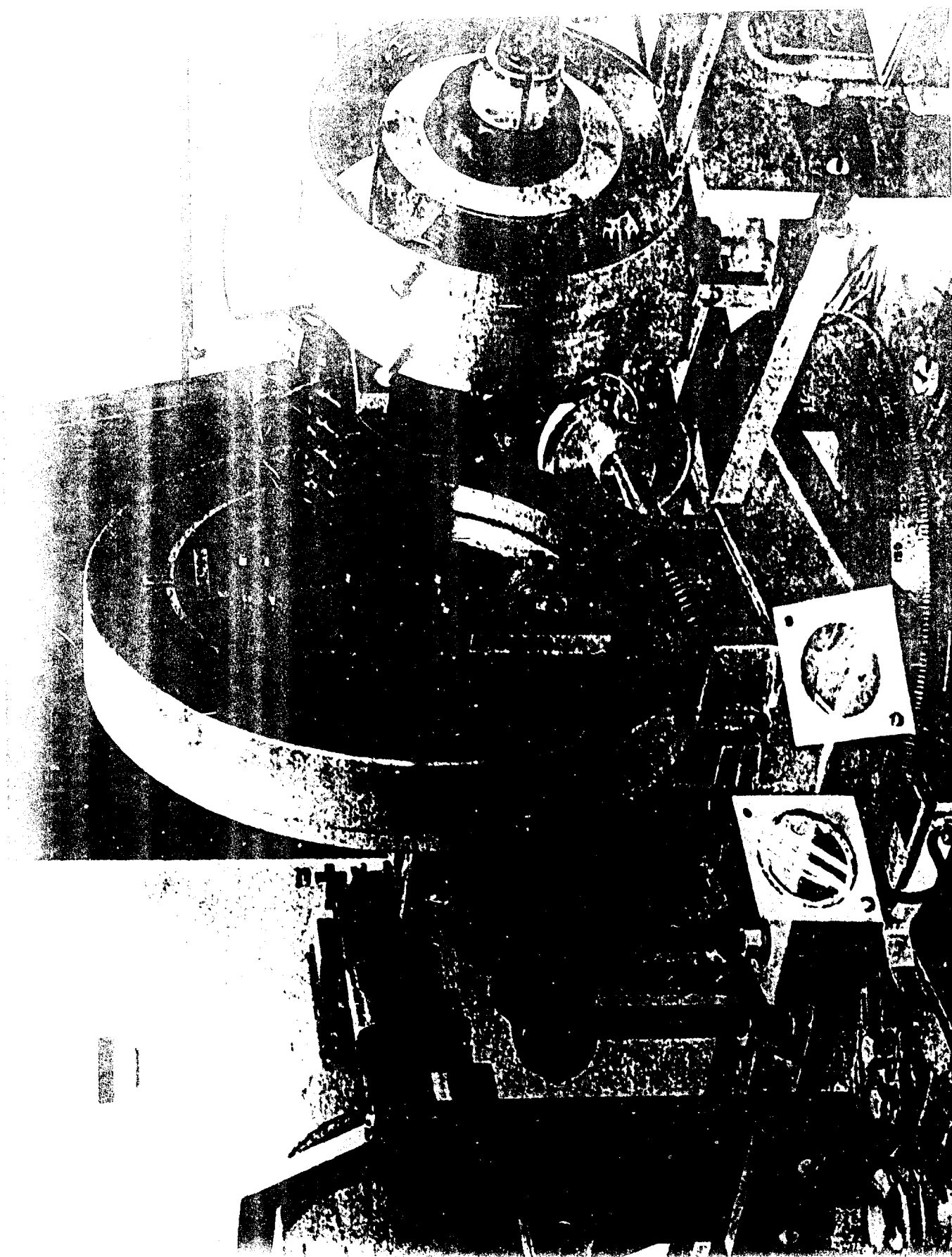


Figure 1

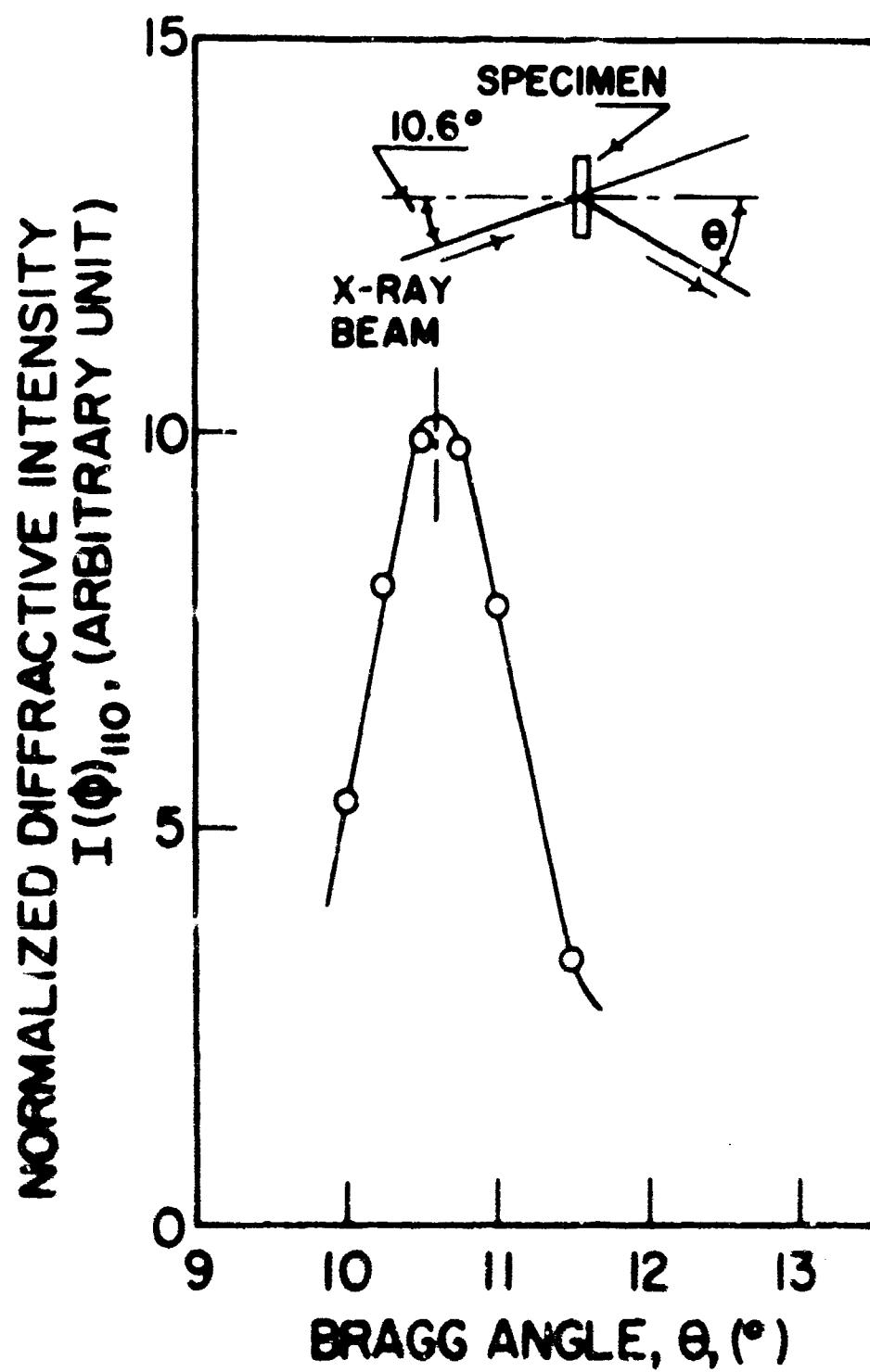


Figure 6



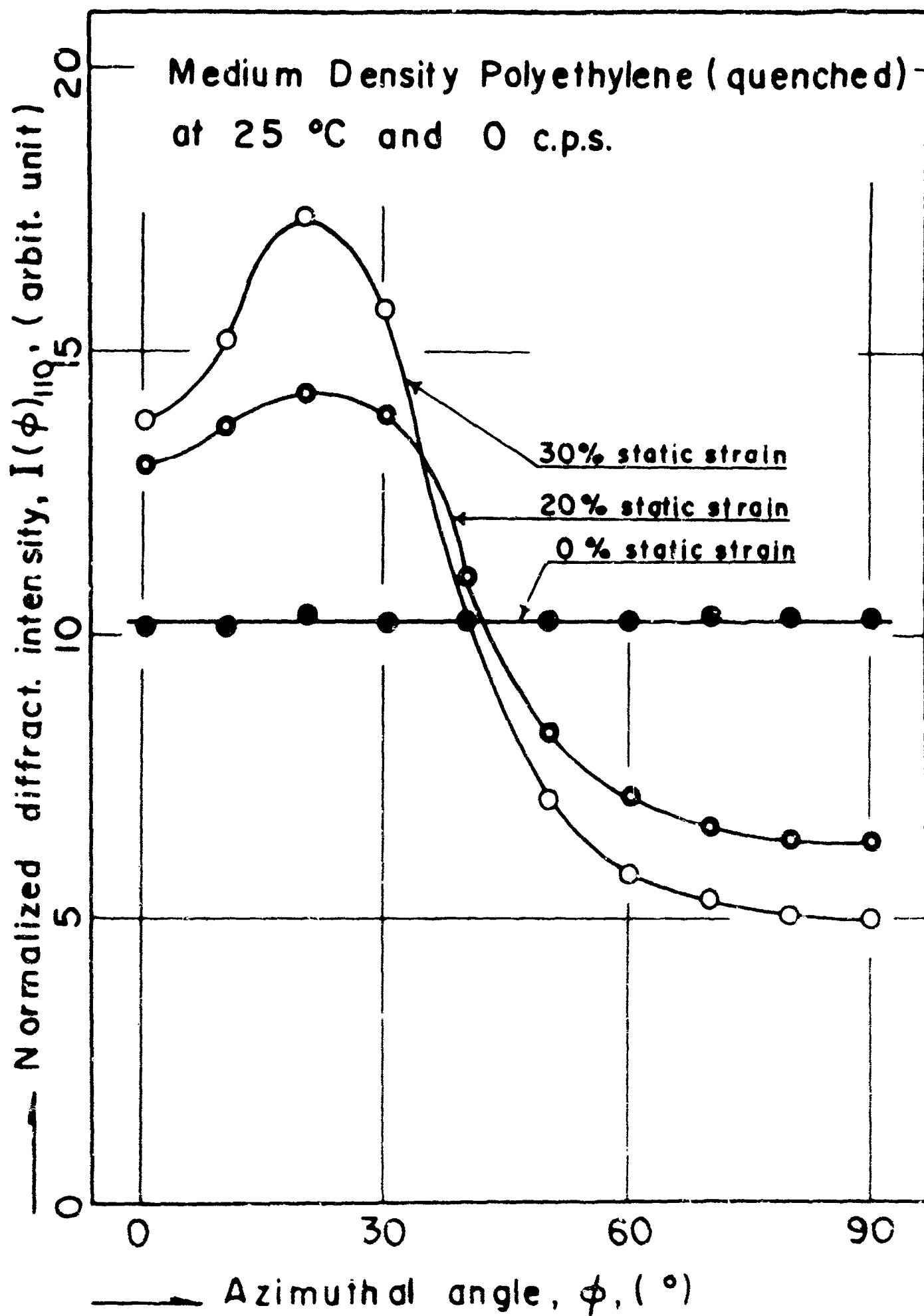


Figure 7

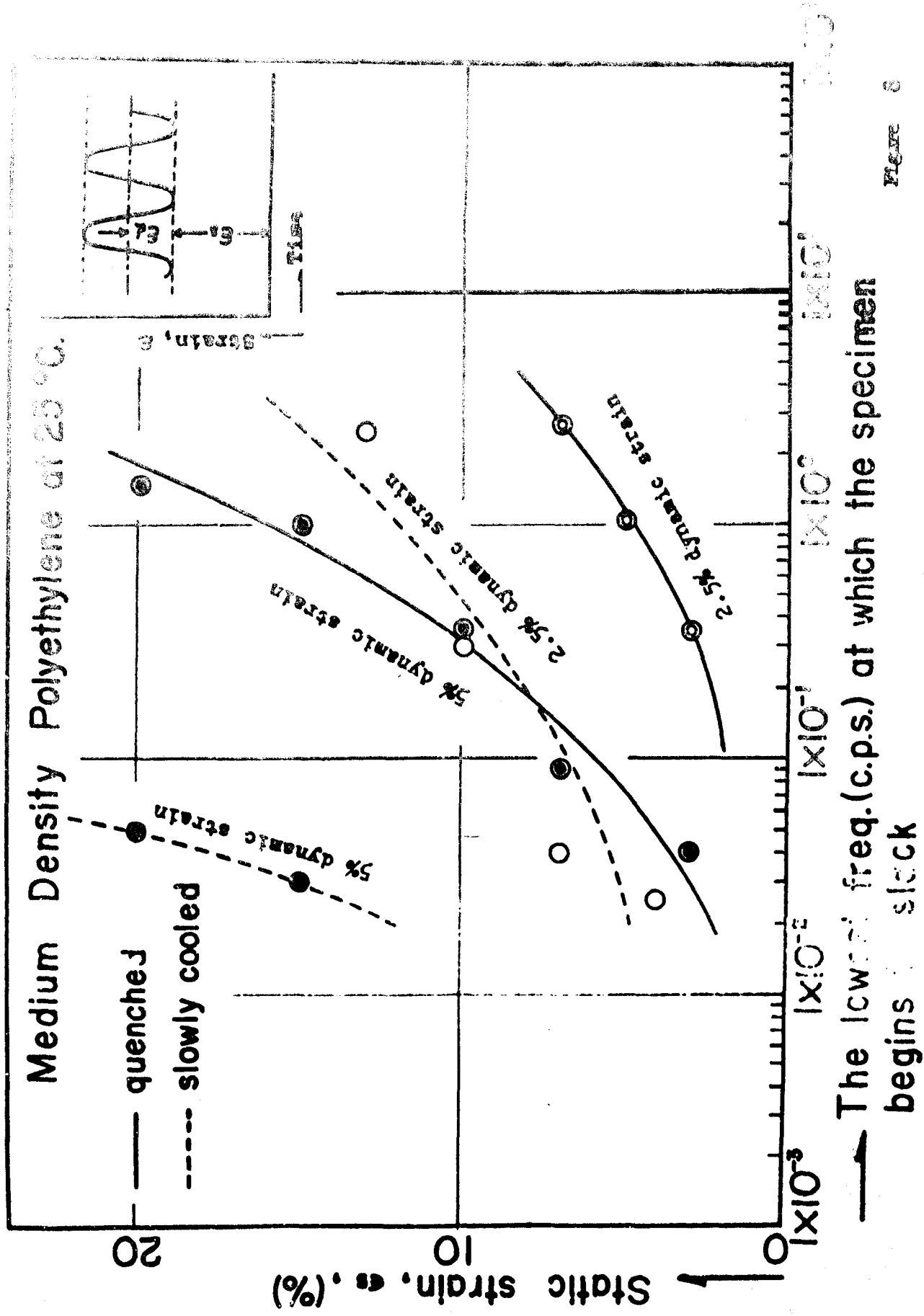


Figure 8

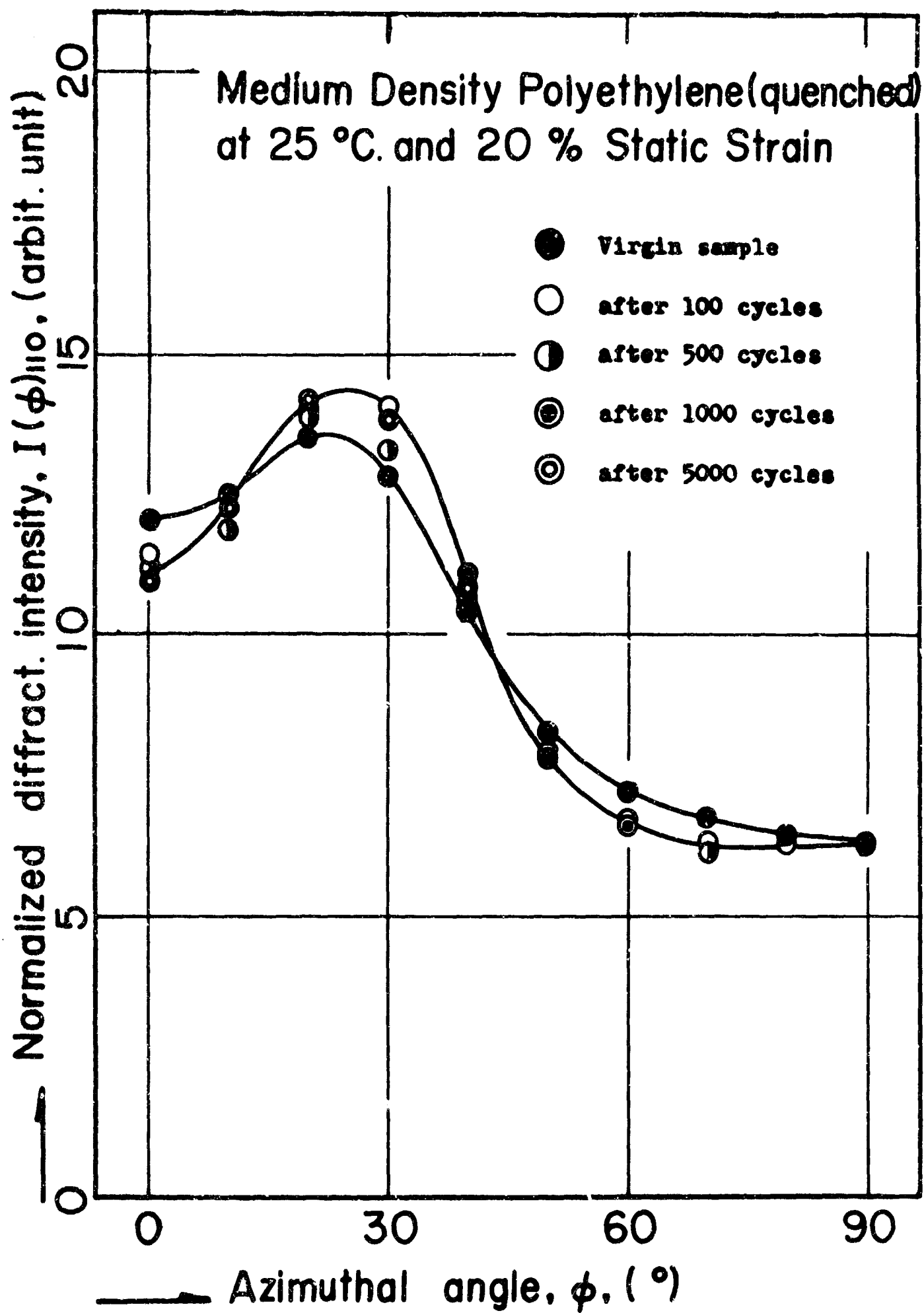


Figure 9

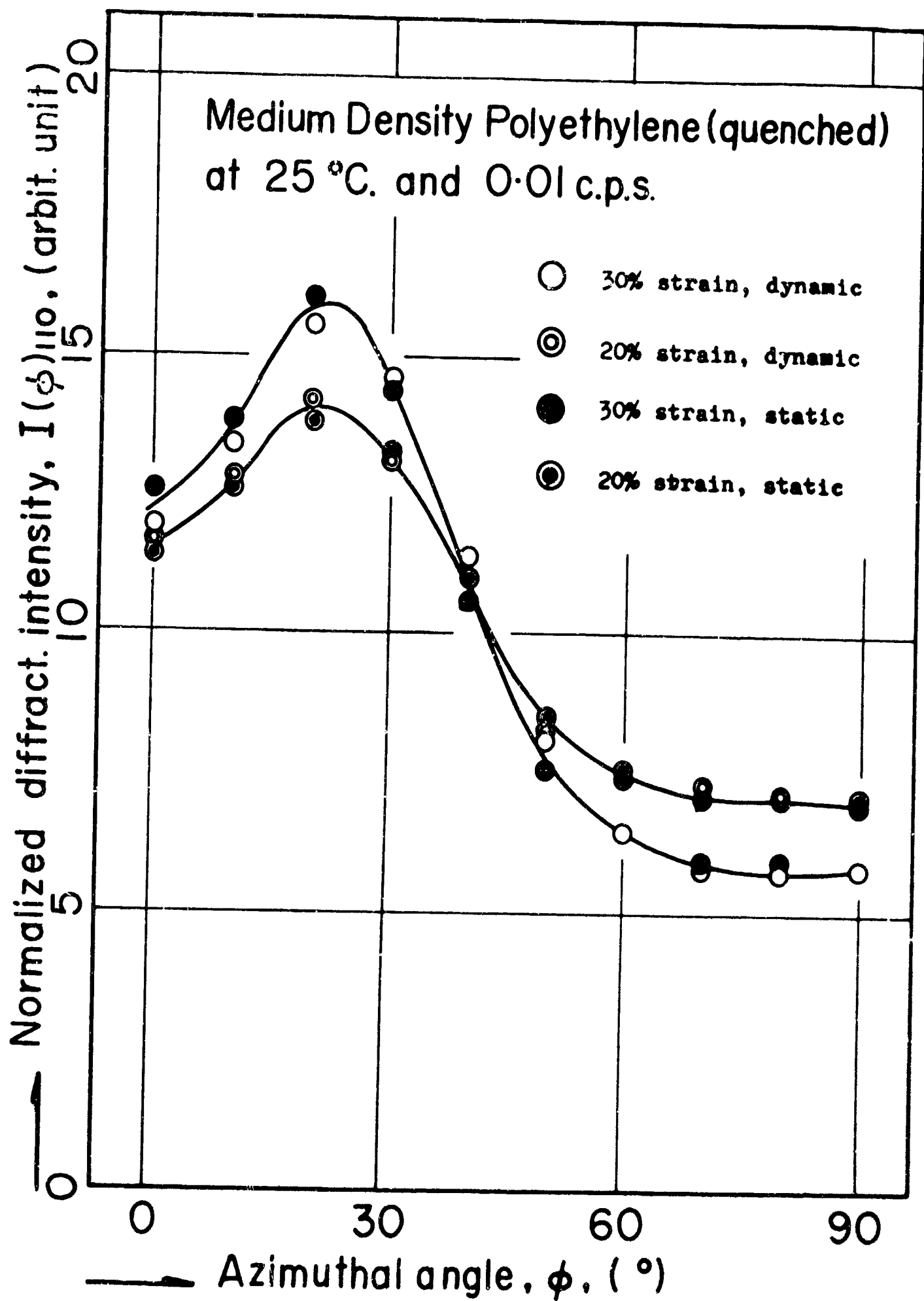


Figure 10

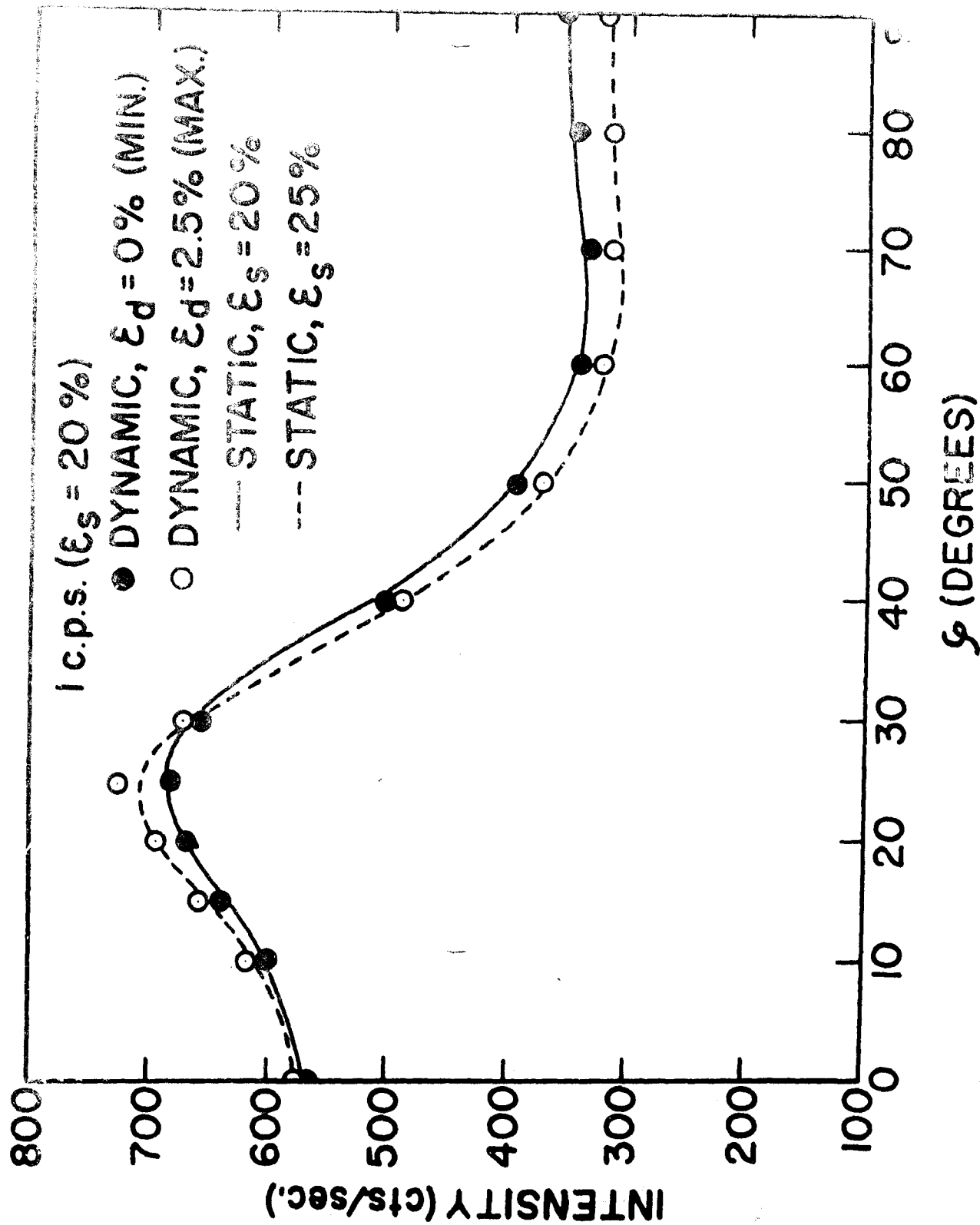


Figure 1

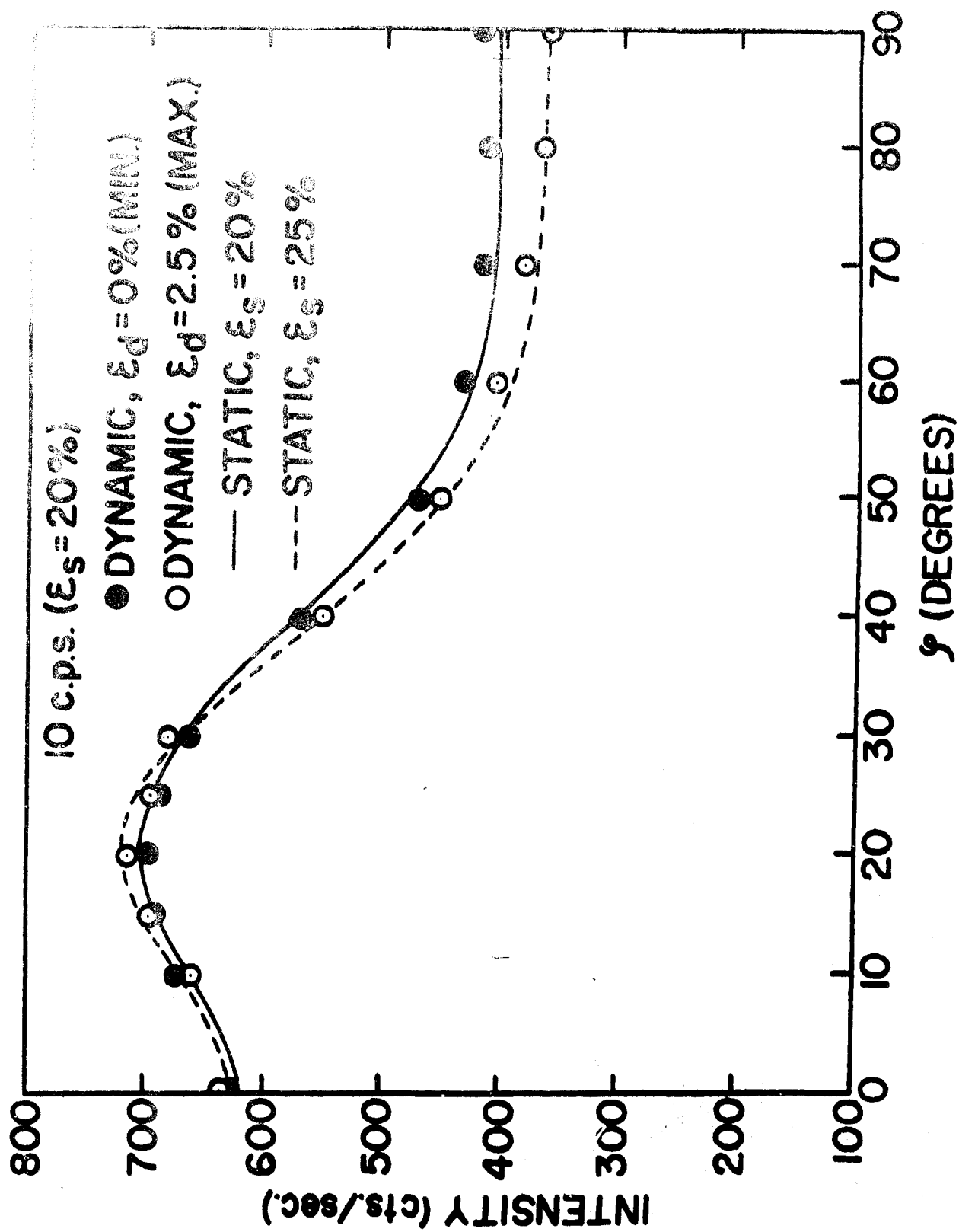


Figure 12

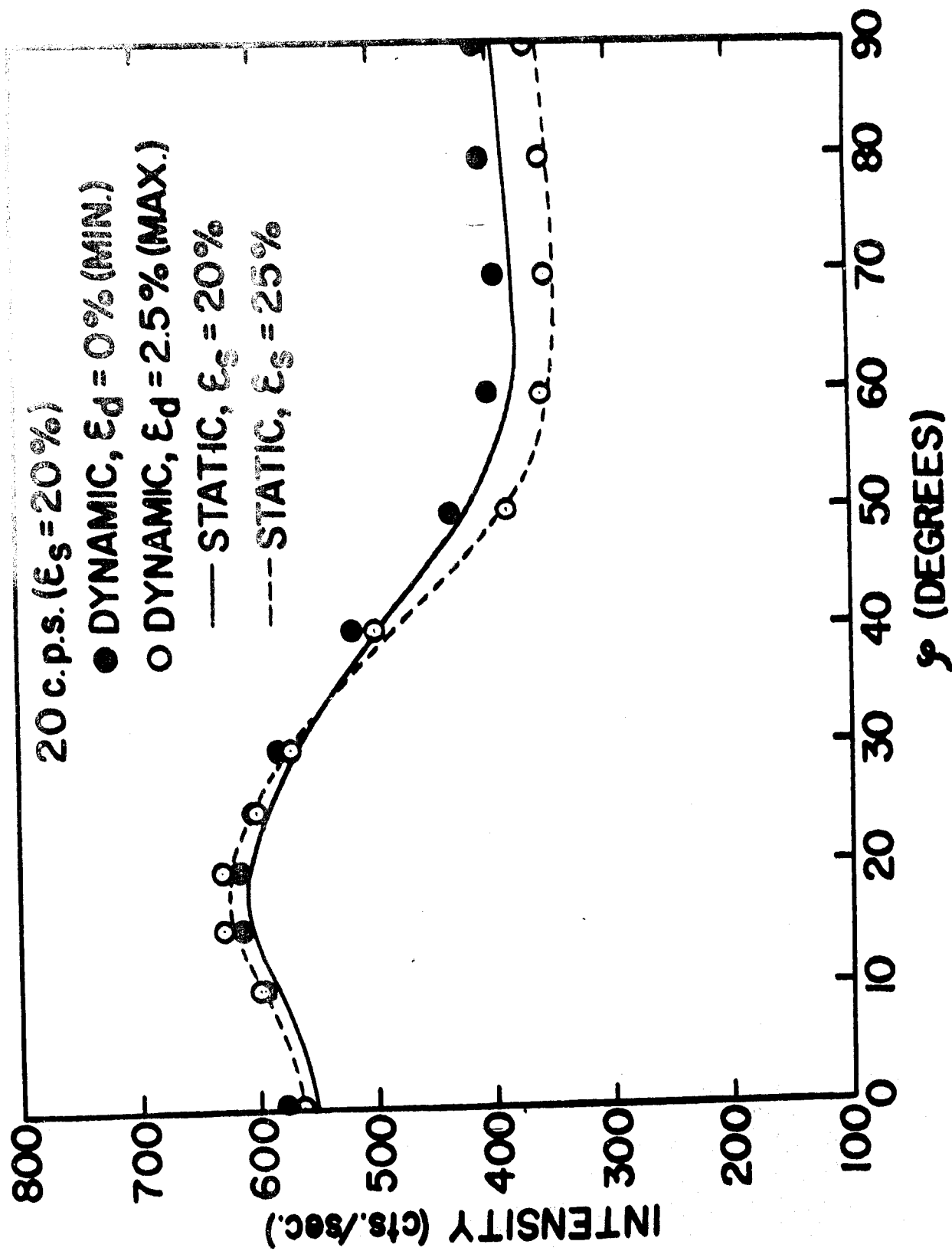


Figure 13

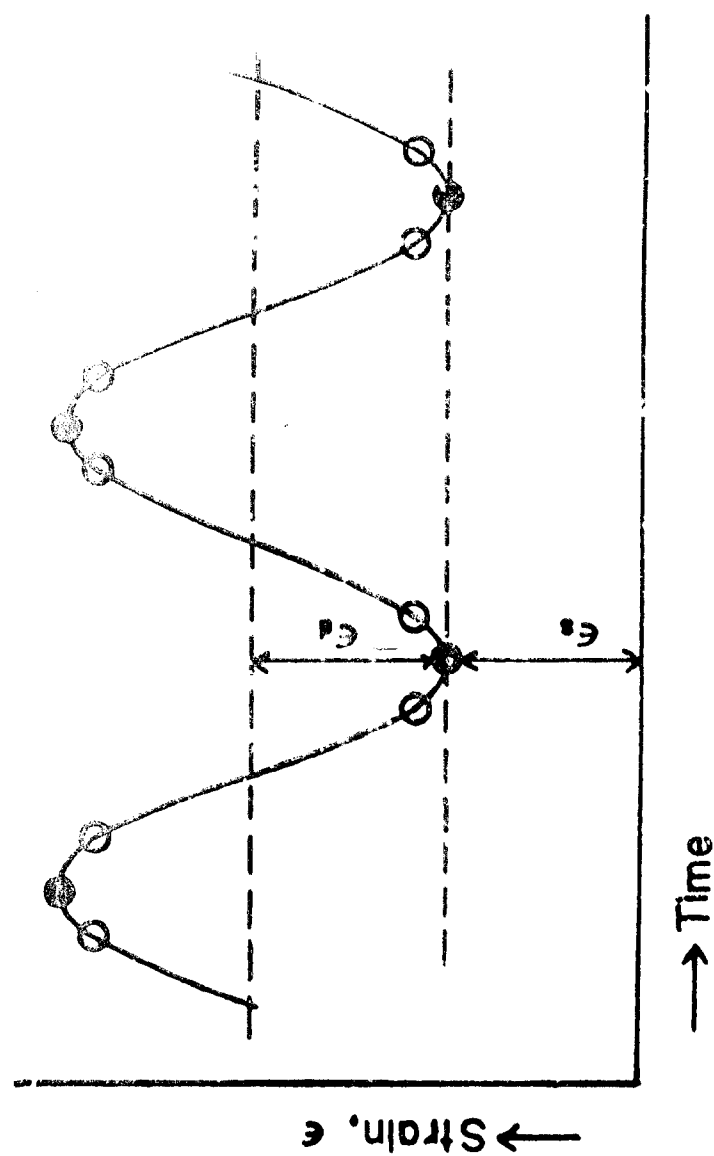
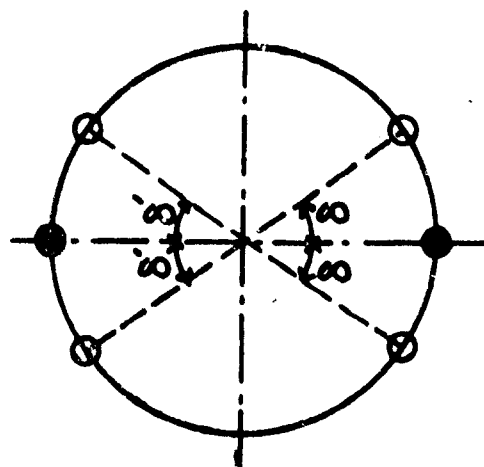


Figure 14